Proceedings of the 3rd International Conference on Mechatronics and Smart Systems
DOI: 10.54254/2755-2721/135/2025.21050

A Novel Type of Micro-channel Heat Sink with Enhanced Thermal-hydraulic Performance by Sawtooth Cross-sectional Shape

Haotian Chen[1,a,*]

[1]*Ann and H.J. Smead Department of Aerospace Engineering Science, University of Colorado Boulder, CO, USA*
a. chenhaotian1121@163.com
**corresponding author*

Abstract: A new shape of cross-section for micro-channel heat sink (MCHS) was designed. The cross-section has a sawtooth boundary. Through numerical simulation, the effects of various geometric parameters, including angle of sawtooth and number of sawtooth, on the MCHS's thermal performance and coolant flow characteristics were explored. According to the results, the cross-section with a sawtooth boundary increases the pressure drop, but at some specific geometric parameters, the heat dissipation performance is enhanced. Thus, the sawtooth cross-section has a better overall thermal performance than the conventional rectangular cross-section for MCHS. After simulating different geometric parameters, it was found that the overall thermal performance is highest when the angle of sawtooth is 30 degrees. Further research based on the 30 degrees angle of sawtooth revealed that when the top and bottom sides have four pairs of sawtooth and the left and right sides have twelve pairs, the overall thermal performance is at its best. Under this optimal configuration, the overall thermal performance of the MCHS with a sawtooth cross-section is 16% higher than that of the MCHS with a traditional rectangular cross-section.

Keywords: micro-channel heat sink, thermal resistance, pumping power, sawtooth cross-sectional shape

1. Introduction

Electronic devices have become much more complicated and require more power in the 21st century. In the era of miniaturization of electronic equipment, the demand for smaller smaller heat dissipation facilities is also growing. Micro-channel heat sinks (MCHS) have attracted interest because of their excellent heat dissipation capabilities and small size. However, in the semiconductor industry, Moore's Law[1] is still in effect: With the help of advanced fabrication technologies, the number of transistors in various chips has increased significantly, leading to an increase in the thermal power of the chip. In addition, the internal architecture of the processor has become more complex, and manufacturing process limitations contribute to uneven temperature distribution within the chip. These factors lead to a decrease in chip lifespan and reliability. Therefore, MCHS also need to improve their overall thermal performance with the iteration of electronic devices.

DOI: 10.54254/2755-2721/135/2025.21050

Numerous studies optimized MCHS with respect to coolants, structures, cross-sectional geometric parameters. Chai et al.[2],Sajid et al.[3],and Liang et al.[4] studied the application of nanofluids, which are currently a popular coolant in thermodynamic area, to strengthen the MCHS's thermal performance. Meanwhile, Vafai et al.[5], Wong et al.[6], and Kumar et al.[7] investigated the impact of the MCHS's structural features, including various inlet and outlet locations and multilayer channels, on the thermal performance of the system. In addition, Marschewski et al.[8], Sajedi et al.[9], and Wang et al.[10] researched the change in thermal performance after adding different shape of pin-fin structure into the MCHS. Finally, some people, such as Hasan et al.[11], Xia et al.[12], and Wang et al.[13], found the effect of channel geometric parameters of the channel on the overall thermal performance of MCHS. These studies demonstrate that MCHS's thermal performance is significantly impacted by the geometric parameters of its cross-section. Therefore, it is reasonable to find a way to improve the thermal performance of MCHS from the geometric parameters of the microchannel cross-section.

This study was based on a traditional rectangular microchannel from one configuration that researched by Wang et al.[13]. By cut-and-fill method, the MCHS cross-section boundary was changed to a sawtooth shape while the section area remains the same. The thermal capacity of the MCHS is enhanced by changing angle of sawtooth and the number of sawtooth on each boundary. By simulating nine different angles of sawtooth and five different numbers of sawtooth, the geometric parameters of the novel type of cross-section with the best overall thermal performance were found.

2. Numerical method

2.1. Governing equations

A three-dimensional conjugate heat transfer model of the MCHS should be established in order to assess the heat transfer within the MCHS as well as the coolant flow. Some simplifications can be made to facilitate the research and reduce the computational cost. Therefore, the following assumptions are made: First, the coolant fluid in the MCHS is stable, incompressible, and single-phase laminar flow. The boundary of the MCHS channel applies to non-slip conditions. Then, radiant heat transfer and the effects of gravitational force are not considered. The properties of solids and liquids are constant. Finally, according to Xu et al.[14], the effect of viscous dissipation can be ignored.

To explain the heat transfer and flow in the MCHS channel, the continuity equation, momentum equation, and fluid energy equation were developed based on these assumptions, as shown in Eqs. (1), (2) and (3):

$$\nabla \cdot \vec{V} = 0 \tag{1}$$

$$\rho_f\left(\vec{V}\nabla \cdot \vec{V}\right) = -\nabla p_f + \mu_f \nabla^2 \vec{V} \tag{2}$$

$$\rho_f C_{p,f}\left(\vec{V}\nabla \cdot T_f\right) = k_f \nabla^2 T_f \tag{3}$$

where $\vec{V}$ is the velocity of fluid, ρ_f is the density of fluid, p_f is the pressure of fluid, μ_f is the dynamic viscosity of fluid, $C_{f,p}$ is the specific heat of the fluid at constant pressure, k_f is the thermal conductivity of the fluid, and T_f is the temperature of fluid.

DOI: 10.54254/2755-2721/135/2025.21050

2.2. Boundary conditions and other mathematical equations

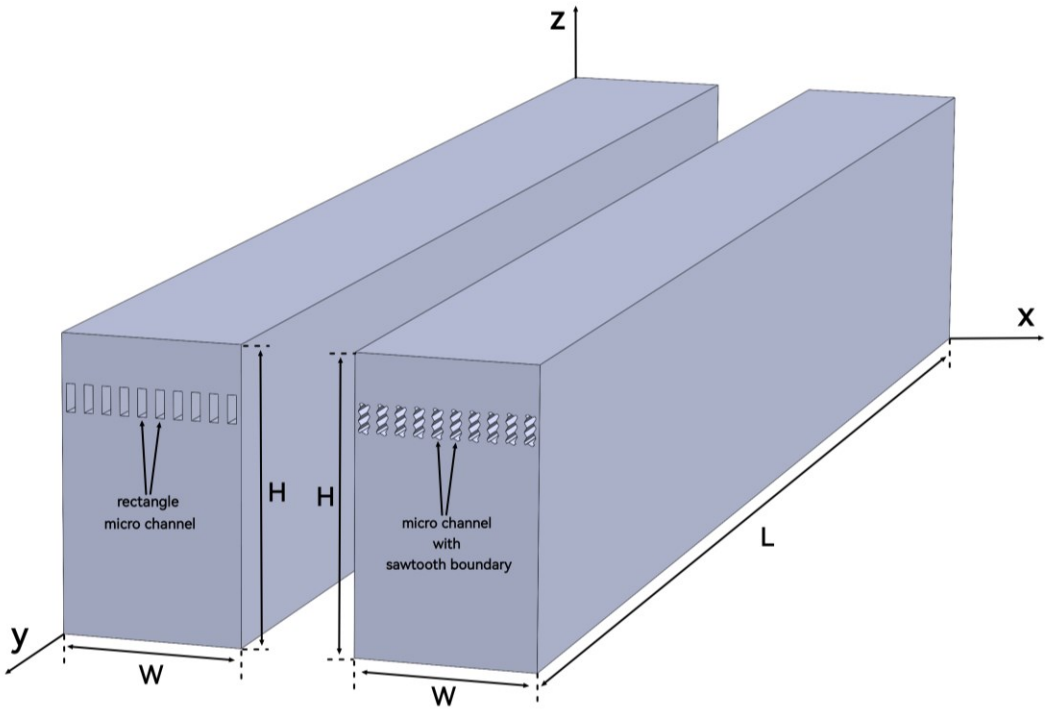

Figure 1: Schematic of the traditional MCHS (left side) and the new MCHS (right side).

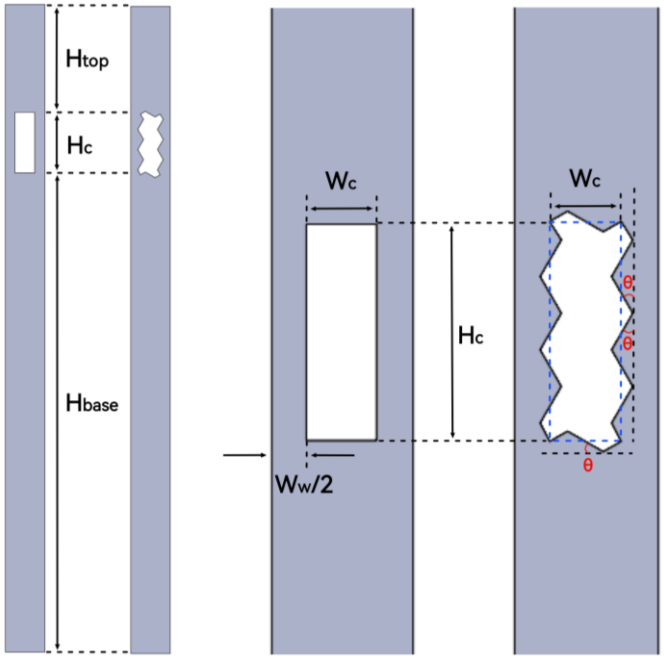

Figure 2: Schematic of cross-section of the MCHS unit.

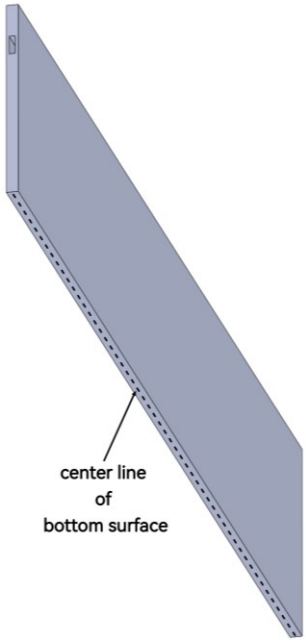

Figure 3: Schematic of temperature measuring line.

The schematic of the traditional MCHS and the new MCHS is shown in Figure. 1. The MCHS on the left have a rectangular channel cross-section, while those on the right have a channel cross-section with sawtooth boundary. A complete MCHS consists of many identical units, so that the results of

DOI: 10.54254/2755-2721/135/2025.21050

numerical simulation of one of units are sufficient to reflect the performance and characteristics of the entire MCHS design. The front views and zoomed schematic for cross-sections of the MCHS units are shown in Figure 2. The new channels were created by the cut-and-fill method: based on rectangular boundary, a concave part was cut and then moved to the other side to form a convex part, thus forming sawtooth boundary. The blue dashed rectangle in the zoomed schematic of the new sections on the right side of Figure 2 is the rectangular boundary before the cut-and-fill method was performed. This method keeps the aspect ratio and cross-sectional area of the duct unchanged.

For better numerical simulation and analysis, a series of boundary conditions were set. In addition, the thermal performance of the new MCHS was compared with that of the MCHS with rectangular channels of Wang et al.[13]. Therefore, some conditions or data were the same as theirs:

(1) The out surfaces of the MCHS unit are fully insulated except for the bottom surface. The bottom surface is in contact with the object that needs heat dissipation, and the constant heat flux is $q_{in} = 100\ W/cm^2$.

(2) Fully developed flow.

(3) The MCHS is made of copper and the coolant is water. The heat is transferred at the contact surface at the boundary of the channel.

(4) The density of copper is 8933 kg m^{-3}, the thermal conductivity of copper is 401 W m^{-1} K^{-1}, the specific heat of copper is 385 J kg^{-1} K^{-1}. The density of copper is 1000 kg m^{-3}, the thermal conductivity of copper is 0.6 W m^{-1} K^{-1}, the specific heat of copper is 4178 J kg^{-1} K^{-1}.

(5) Before the cut-and-fill method, the channel width, W_c, is 0.231 mm, the channel height, H_c, is 0.713 mm, and the total thickness of two walls on left and right side, W_w, is 0.236 mm.

(6) The reference pressure is 1 atm.

(7) The inlet temperature of coolant, T_{in}, is 288.15 K

(8) The inlet velocity is determined by the Reynolds number, which is fixed at Re = 600 in this study.

In order to compare the traditional MCHS with rectangle channel and the new MCHS with sawtooth channel, some calculations were necessary. First, the hydraulic diameter and the inlet velocity can be calculated using Eqn. (4), (5), and (6):

$$D_h = \frac{4A_c}{P_c} = \frac{4W_cH_c}{P_c} \tag{4}$$

$$Re = \frac{\rho_f V_{in} D_h}{\mu_f} \tag{5}$$

$$V_{in} = \frac{Re\mu_f}{\rho_f D_h} \tag{6}$$

where A_c is the area of channel cross-section, P_c is the perimeter of channel cross-section, W_c is the width of channel, H_c is the height of channel, Re is the Reynolds number, ρ_f is the density of fluid, V_{in} is the velocity of fluid at inlet of channel, D_h is the hydraulic diameter, and μ_f is the dynamic viscosity of fluid.

Then, the heat transfer coefficient, pumping power thermal resistance, and figure of merit (FOM) were calculated. As shown in Eqn. (7), (8), (9), and (10). These equations were obtained from Hajmohammadi et al.[15]. These are important parameters to compare the thermal performance of MCHS.

$$h = \frac{q_{in}}{(\overline{T}_b - T_{in})} \tag{7}$$

$$\Omega = \dot{Q}\Delta P = A_c V_{in} \Delta P \tag{8}$$

DOI: 10.54254/2755-2721/135/2025.21050

$$R = \frac{T_{max} - T_{min}}{Q} = \frac{T_{max} - T_{in}}{A_b q_{in}} \tag{9}$$

$$FOM = \frac{\frac{h_{new}}{h_{ref}}}{\left(\frac{P_{new}}{P_{ref}}\right)^{\frac{1}{3}}} \tag{10}$$

where q_{in} is the heat flux into the channel, $\overline{T}_b$ is the average temperature of center line on the bottom surface as shown in Figure 3, and T_{in} is the inlet coolant temperature, $\dot{Q}$ is the volume flow rate, ΔP is the pressure drop from channel's inlet to outlet, T_{max} is the maximum temperature of channel, $T_{min}(=T_{in})$ is the minimum temperature of channel, Q is the heat into channel, A_b is the area of bottom surface, h_{new} is the heat transfer coefficient of new cases (sawtooth channel), h_{ref} is the heat transfer coefficient of reference cases (rectangle channel), P_{new} is the pumping power of new cases, and P_{ref} is the pumping power of reference cases.

2.3. Model validation and grid test

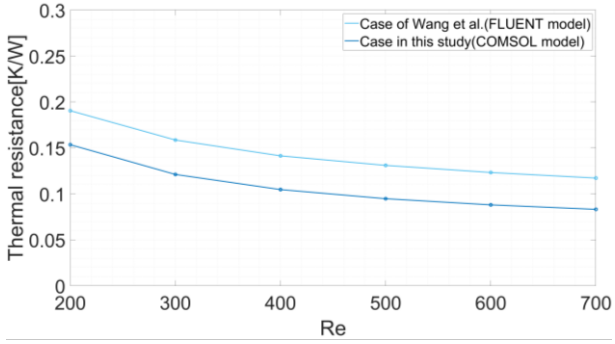

Figure 4: Relationship between thermal resistance and Reynolds number.

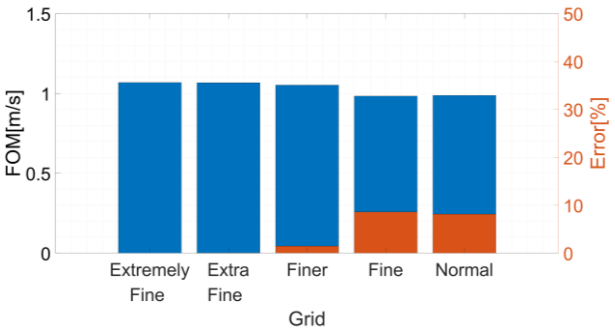

Figure 5: Grid test.

Figure 4 illustrates how thermal resistance varies with Reynolds number from the reference case of Wang et al.[13] and the case in this study. The aspect ratio of the channel, α, are both 3.087 in these cases. There is a difference in the absolute value on the data due to the difference in grid density and the difference in assumptions. However, the trend of the relationship in the two case are consistent. Therefore, it can be considered that the model in this study is valid.

This study used the finite element method to simulate the flow inside the channel. Five different default grid densities in the simulation software, from "Extremely Fine" to "Normal", were tested and the results are shown in Figure 5. The difference between the "Finer" and "Extremely Fine" grids is within 5%, while the difference between the "Fine" and "Extremely Fine" grids is near 10%.

DOI: 10.54254/2755-2721/135/2025.21050

Therefore, the "Finer" grid was used for simulation in order to balance computational cost and simulation accuracy.

3. Results and discussion

3.1. Effect of the sawtooth parameter on thermal performances

3.1.1. Effect of the angle of sawtooth on thermal performances

In this section, the boundary of the channel was modified to sawtooth shapes. The effect of the angle of sawtooth, the θ as shown in Figure 2, on the thermal performance was simulated. In this section, there are three pairs of sawtooth on the left and right sides and one pair on the top and bottom sides.

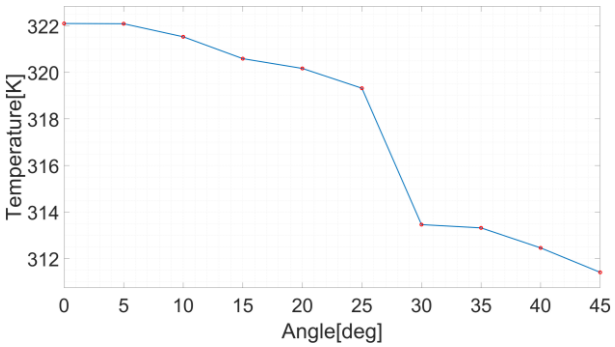

Figure 6: Relationship between average temperature at center line on the bottom surface and angle of sawtooth.

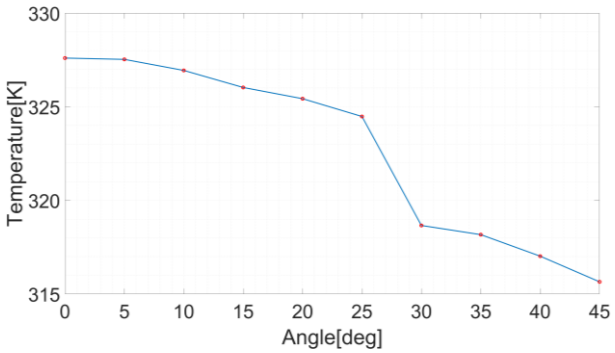

Figure 7: Relationship between max and angle of sawtooth.

Figure 6 demonstrates the relationships between the average temperature at bottom surface's center line and the sawtooth angle, and the relationship between the max temperature of MCHS and the angle of sawtooth is shown in Figure 7. When the channel is rectangular (θ = 0°), both the average temperature at bottom surface's center line, $\overline{T}_b$, and the maximum temperature of the entire MCHS, T_{max}, are at their maximum, while $\overline{T}_b = 322.1$ K, and $T_{max} = 327.6$ K. As θ increases, both $\overline{T}_b$ and T_{max} show decreasing trend. When 0°<θ<25° and 30°<θ<45°, the temperature decreases slowly with an increase in θ. When 25°<θ<30°, the temperature drops more sharply. When θ = 45°, both temperatures reach their minimum, while $\overline{T}_b = 311.4$ K and $T_{max} = 315.7$K.

DOI: 10.54254/2755-2721/135/2025.21050

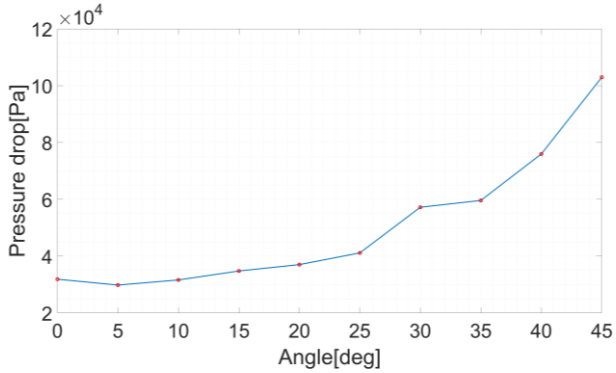

Figure 8: Relationship between pressure drop and angle of sawtooth.

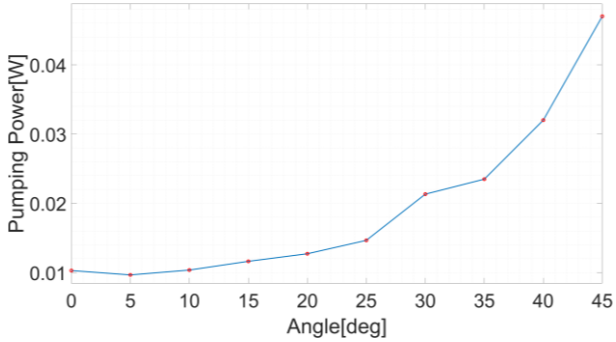

Figure 9: Relationship between pumping power and angle of sawtooth.

Figure 8 shows the relationship between pressure drop and angle of sawtooth, while Figure 9 shows the relationship between pumping power and angle of sawtooth. When the channel is rectangular ($\theta = 0°$), both the pressure drops, ΔP, and the pumping power, Ω, have relatively low values, while $\Delta P = 31874$ Pa, and $\Omega = 0.010291$ W. As θ increases, both ΔP and Ω show increasing trend. When $0° < \theta < 25°$ and $30° < \theta < 35°$, the ΔP and Ω increases slowly with an increase in θ. When $25° < \theta < 45°$ and $50° < \theta < 45°$, the ΔP and Ω increases more sharply. When $\theta = 45°$, both ΔP and Ω reach their maximum, while $\Delta P = 102968$ Pa and $\Omega = 0.047012$ W.

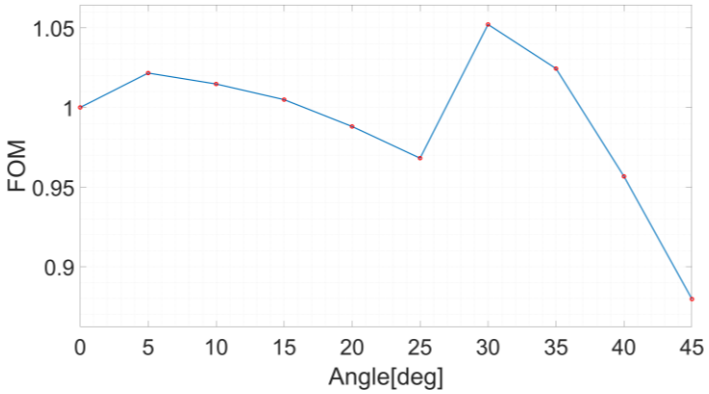

Figure 10: Relationship between FOM and angle of sawtooth.

As shown in Figure 10, the FOM for the reference case (the channel is rectangular) is 1. The FOM increases significantly as the sawtooth angle rises from 0° to 5°. When $5°<\theta<25°$, the FOM slowly decreases with increasing angle. When the angle of sawtooth changes from 25° to 30°, the FOM

DOI: 10.54254/2755-2721/135/2025.21050

experiences a sharp increase again. At θ=30°, FOM reaches its maximum value, while FOM = 1.0521. When 30°<θ<45°, FOM decreases sharply. At θ=45°, FOM reaches its minimum value, while FOM=0.87966.

3.1.2. Effect of the number of sawtooth on thermal performances

In this section, θ is set to 30° uniformly, which is when FOM reaches its maximum value in the previous section. It would be investigated how the amount of sawtooth affects thermal performance. The number of pairs of sawtooth (one convex part and one concave part) on the top and bottom sides is set to N. Since the aspect ratio of the channel is about , when there are N pairs of sawtooth on the top and bottom edges, there are 3N pairs of serrations on the left and right edges.

Figure 11: Relationship between average temperature at center line on the bottom surface and number of sawtooth.

Figure 12: Relationship between max temperature and number of sawtooth.

The relationship between the average temperature at center line of bottom surface and the number of sawtooth is shown in Figure 11, and the relationship between the max temperature of MCHS and the number of sawtooth is shown in Figure 12. When channel is rectangular (N=0), both $\overline{T}_b$, and T_{max}, are at their maximum, while $\overline{T}_b = 322.1$ K, $T_{max} = 327.6$ K. As N increases from 0 to 1, the temperature decreases rapidly. When 1<N<4, both temperatures gradually increase with the increase of N. When N=1, both $\overline{T}_b$ and T_{max} reach their minimum, while $\overline{T}_b = 313.46$ K, $T_{max} = 318.66$ K.

DOI: 10.54254/2755-2721/135/2025.21050

Figure 13: Relationship between pressure drop and number of sawtooth.

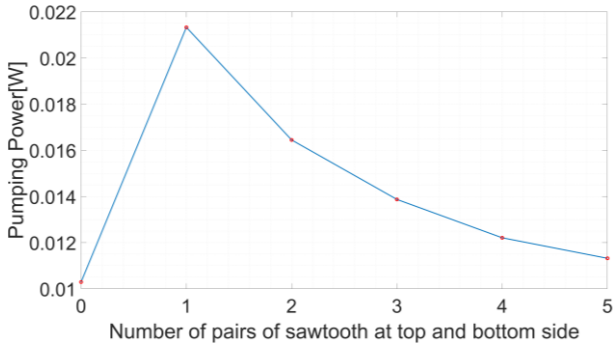

Figure 14: Relationship between pumping power and number of sawtooth.

The relationship between the pressure drop and the number of sawtooth is shown in Figure 13, and the relationship between the pumping power and the number of sawtooth is shown in Figure 14. When N increases from 0 to 1, both ΔP and Ω increase rapidly. When 1<N<4, both ΔP and Ω gradually decrease with increasing N. When N=1, both ΔP and Ω are at their maximum, while $\Delta P = 57206$ Pa and $\Omega = 0.021326$ W. When N=5, both ΔP and Ω are at their minimum, while $\Delta P = 30364$ Pa and $\Omega = 0.011319$ W.

Figure 15: Relationship between FOM and number of sawtooth.

As shown in the Figure 15, when N=0 for reference case, the FOM is 1. When 1<N<4, the FOM increases with increasing N. When N=4, the FOM reaches its maximum value, while FOM=1.1612. Then, the FOM starts to decrease with increasing N.

DOI: 10.54254/2755-2721/135/2025.21050

3.2. Comparison of the new MCHS with the traditional MCHS

It can be seen from the data in section 3.1 that both the angle of sawtooth and the number of sawtooth have a immense effect on the temperature, pressure drop, pumping power, and FOM. The FOM aptly describes the MCHS's overall thermal performance because it was computed using the pumping power and the heat transfer coefficient.

When considering the angle of sawtooth, the FOM exceeds 1 for both $0°<\theta<15°$ and $30°<\theta<35°$, which means that the overall thermal performance of the channel with sawtooth cross-section is better than that of the channel with rectangular cross-section in these angle ranges. If only the heat dissipation, or temperature, is considered, all sawtooth channels are better than rectangular channels. Meanwhile, when $\theta>5°$, the sawtooth channel's pressure drop and pumping power are higher than those of the rectangular channel. which is bad for the overall thermal performance. The optimal option, where the FOM reaches its maximum, is $\theta=30°$, when heat dissipation and pumping power are traded off.The FOM of all five sawtooth channels is greater than 1 when the variation in the number of sawtooth counts is taken into account, indicating that they outperform the rectangular channel in terms of overall thermal performance. If only considering heat dissipation,, all sawtooth channels are better than the rectangular channel. Meanwhile, when $1<N<5$, the pressure drop and the pumping power of the sawtooth channel is larger than that of the rectangular channel. Similarly, if a trade-off is made between heat dissipation and pumping power, then $N=4$ is the best solution, where the FOM reaches its maximum value.

3.3. Mechanism behind the performance

3.3.1. Effect of the angle of sawtooth on thermal performances

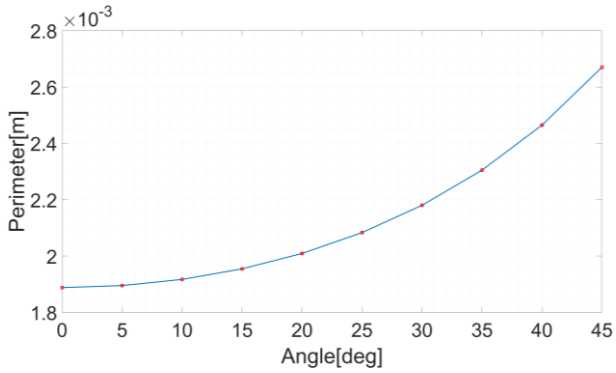

Figure 16: Relationship between perimeter of velocity cross section and angle of sawtooth.

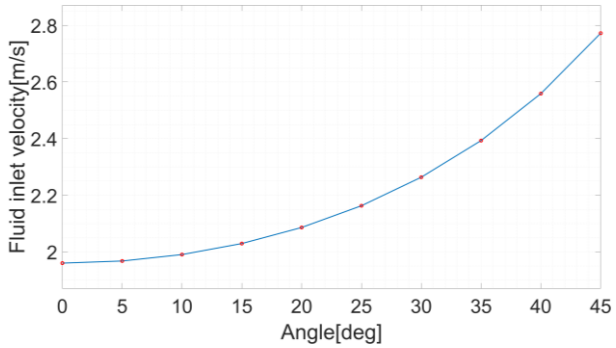

Figure 17: Relationship between fluid inlet and angle of sawtooth.

DOI: 10.54254/2755-2721/135/2025.21050

First, as shown in Figure 16 and Figure 17, under a constant Reynolds number (the Reynolds number was set to 600 in this study), the inlet perimeter increased due to the increasing angle of sawtooth, then the fluid inlet velocity also increased with the increase of the angle of sawtooth.

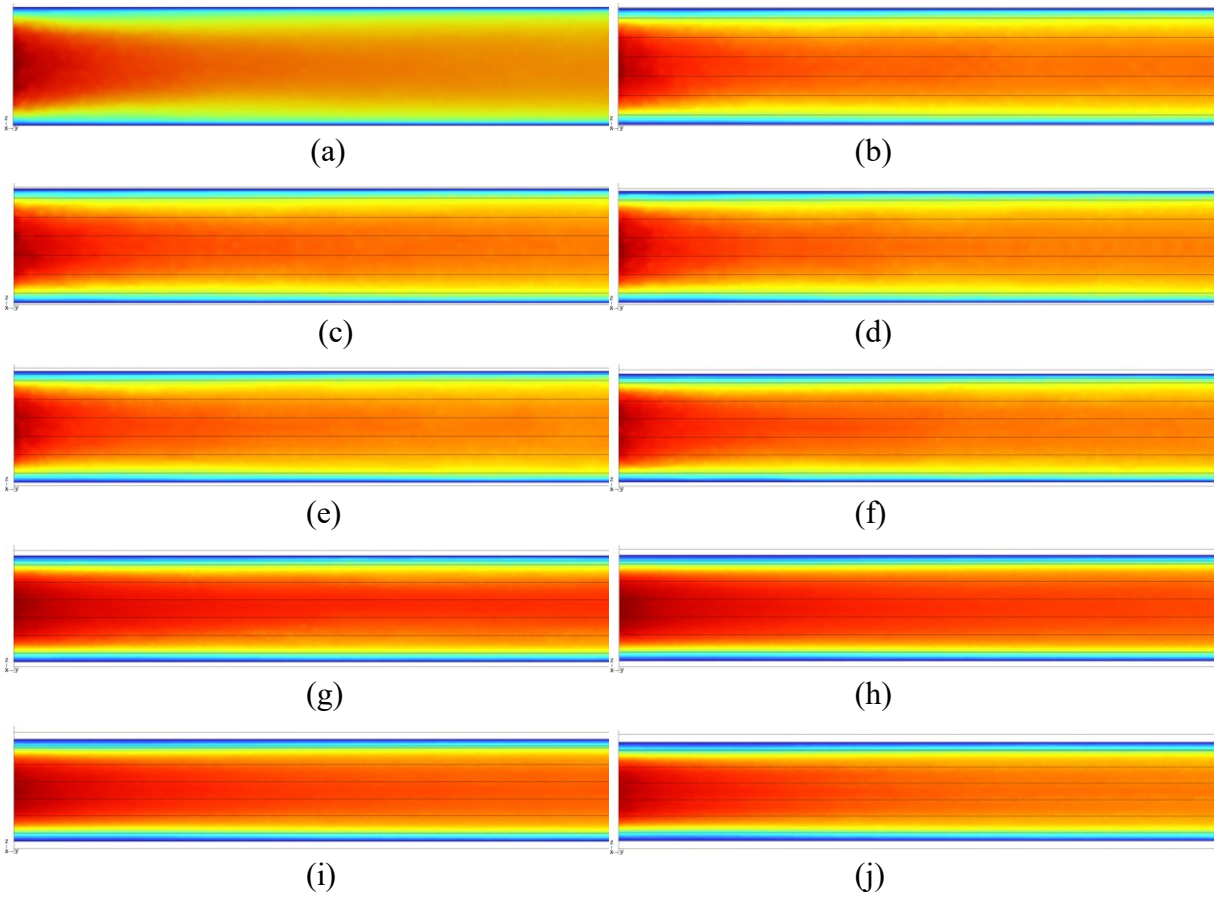

Figure 18: The diagram of velocity of coolant along the channel at different angle of sawtooth. (a) θ=0°; (b) θ=5°; (c) θ=10°; (d) θ=15°; (e) θ=20°; (f) θ=25°; (g) θ=30°; (h) θ=35°; (g) θ=30°; (h) θ=35°; (i) θ=40°; (j) θ=45°.

As stated in Section 3.1.1, the average temperature of the center line at the MCHS's bottom surface or maximum temperature of the entire MCHS drops as the angle of sawtooth increases, while the pressure drop and pumping power rise. Figure 18 displays the velocity diagram at the channel's central cut surface for various sawtooth angles. The thickness of the boundary layer in the sawtooth channel is more stable than in the rectangle channel (θ=0°), and compared to the rectangular channel, the sawtooth channel experiences a slower mixing of boundary layer and mainstream. It is possible that the additional area of the sawtooth boundary provides greater viscous forces to maintain the boundary layer. Moreover, there are stable turbulences at the interface between the boundary layer and the mainstream in the sawtooth channel, which improves heat transfer. Moreover, the higher inlet velocity of flow causes the volume flow rate to rise as well, aiding in heat transfer; nevertheless, the pressure drop also rises concurrently. When θ increases to 30°, as shown in Figure 18(g), the yellow layer in the diagram thins out, which also means that the size of turbulent begins to decrease and the thickness of the boundary layer becomes thinner. Although the heat transfer performance can be further improved, the higher sawtooth will cause the pressure drop to increase rapidly, causing the FOM value to begin to decrease instead.

DOI: 10.54254/2755-2721/135/2025.21050

3.3.2. Effect of the number of sawtooth on thermal performances

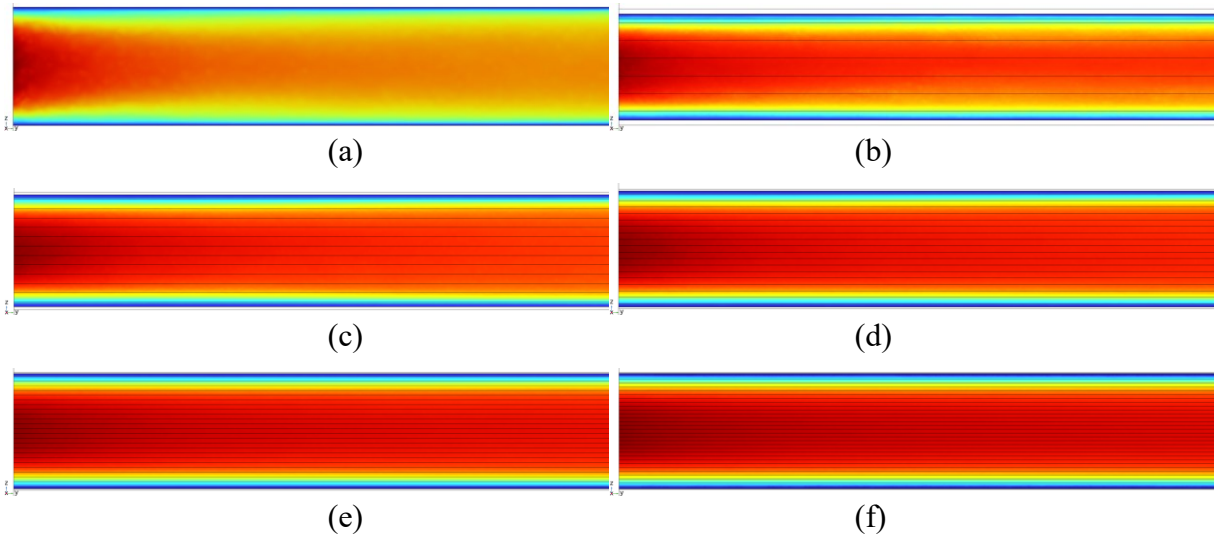

Figure 19: The diagram of velocity of coolant along the channel at different number of sawtooth. (a) N=0; (b) N=1; (c) N=2; (d) N=3; (e) N=4; (f) N=5.

As described in section 3.1.2, with an increase in the number of sawtooth, both the average average temperature of the center line at the MCHS's bottom surface and the maximum temperature of the MCHS increase. And the pressure drop and pumping power also decreases. The velocity diagram at the channel's central cut surface for various number of sawtooth as shown in Figure 19. As can be seen from Figure 19(a) and Figure 19(b), the thickness of the boundary layer for sawtooth channel becomes thinner and is more stable than that of the rectangular channel, which is generally similar to the conditions described in previous section. However, since the change in the number of sawtooth does not lead to a change in the cross-sectional area, the inlet velocity of the flow is constant. From Figure 19(b) to Figure 19 (f), the deep red area in the center of the channel becomes longer, while the number of sawtooth increases, which means that the central flow velocity decreases more slowly. Because at the constant angle of sawtooth, the more sawtooth means a lower sawtooth height, which is beneficial for maintaining the central flow velocity and removing more heat.

4. Conclusions

A new type of MCHS cross-section with sawtooth boundary was designed by a cut-and-fill method based on the traditional rectangular cross-section, under the prerequisite that the aspect ratio and cross-sectional area of the channel remain unchanged. Through numerical modeling, the impact of angle and number of sawtooth on the MCHS's overall thermal performance was also examined. The following are the primary conclusions:

(1) As the angle of sawtooth increases, the temperature of MCHS decreases, and the temperature reaches its minimum when the angle of sawtooth reaches 45 degrees. In addition, when the angle of sawtooth is the same, an increase in the number of sawtooth leads to an increase in the temperature. When there are 5 pairs of sawtooth on the top and bottom sides and 15 pairs on the left and right sides, the temperature reaches the highest temperature in the new MCHS, but it is still lower than that in the traditional MCHS.

(2) As the angle of sawtooth increases, the pumping power and pressure drop of MCHS increases, and both pressure drop and pumping power reach its maximum when the angle of sawtooth reaches 45 degrees. Meanwhile, when the angle of sawtooth is the same, an increase in the number of sawtooth

leads to an decrease in the pressure drop and pumping power. When there are 5 pairs of sawtooth on the top and bottom sides and 15 pairs on the left and right sides, the pumping power and pressure drop reaches the minimum in the new MCHS.

(3) The overall thermal performance of these channels is evaluated by FOM, a parameter that takes into account both pumping power and heat transfer coefficient of the MCHS. When the angle of the sawtooth is 30 degrees, there are 4 pairs of sawtooth on the top and bottom sides, and 12 pairs on the left and right sides, the sawtooth channel has the best performance, which the FOM is 1.1612, which means the overall thermal performance of the new MCHS in this condition is improved by about 16% compared with the traditional MCHS.

References

[1] *Moore, G. E. (1998). Cramming more components onto integrated circuits. Proceedings of the IEEE, 86(1), 82–85. https://doi.org/10.1109/jproc.1998.658762*

[2] *Chai, L., Shaukat, R., Wang, L., & Wang, H. S. (2018). A review on heat transfer and hydrodynamic characteristics of Nano/microencapsulated phase change slurry (N/MPCS) in Mini/Microchannel Heat Sinks. Applied Thermal Engineering, 135, 334–349. https://doi.org/10.1016/j.applthermaleng.2018.02.068*

[3] *Sajid, M. U., & Ali, H. M. (2019). Recent advances in application of nanofluids in heat transfer devices: A critical review. Renewable and Sustainable Energy Reviews, 103, 556–592. https://doi.org/10.1016/j.rser.2018.12.057*

[4] *Liang, G., & Mudawar, I. (2019). Review of single-phase and two-phase nanofluid heat transfer in macro-channels and micro-channels. International Journal of Heat and Mass Transfer, 136, 324–354. https://doi.org/10.1016/j.ijheatmasstransfer.2019.02.086*

[5] *Vafai, K., & Zhu, L. (1999). Analysis of two-layered micro-channel heat sink concept in electronic cooling. International Journal of Heat and Mass Transfer, 42(12), 2287–2297. https://doi.org/10.1016/s0017-9310(98)00017-9*

[6] *Wong, K.-C., & Ang, M.-L. (2017). Thermal hydraulic performance of a double-layer microchannel heat sink with channel contraction. International Communications in Heat and Mass Transfer, 81, 269–275. https://doi.org/10.1016/j.icheatmasstransfer.2016.09.013*

[7] *Kumar, R., Singh, G., & Mikielewicz, D. (2019). Numerical Study on mitigation of flow maldistribution in parallel microchannel heat sink: Channels variable width versus variable height approach. Journal of Electronic Packaging, 141(2). https://doi.org/10.1115/1.4043158*

[8] *Marschewski, J., Brechbühler, R., Jung, S., Ruch, P., Michel, B., & Poulikakos, D. (2016). Significant heat transfer enhancement in microchannels with Herringbone-inspired microstructures. International Journal of Heat and Mass Transfer, 95, 755–764. https://doi.org/10.1016/j.ijheatmasstransfer.2015.12.039*

[9] *Sajedi, R., Osanloo, B., Talati, F., & Taghilou, M. (2016). Splitter plate application on the circular and square pin fin heat sinks. Microelectronics Reliability, 62, 91–101. https://doi.org/10.1016/j.microrel.2016.03.026*

[10] *Wang, Y., Shin, J.-H., Woodcock, C., Yu, X., & Peles, Y. (2018). Experimental and numerical study about local heat transfer in a microchannel with a pin fin. International Journal of Heat and Mass Transfer, 121, 534–546. https://doi.org/10.1016/j.ijheatmasstransfer.2018.01.034*

[11] *Hasan, M. I., Rageb, A. A., Yaghoubi, M., & Homayoni, H. (2009a). Influence of channel geometry on the performance of a counter flow microchannel heat exchanger. International Journal of Thermal Sciences, 48(8), 1607–1618. https://doi.org/10.1016/j.ijthermalsci.2009.01.004*

[12] *Xia, G., Ma, D., Zhai, Y., Li, Y., Liu, R., & Du, M. (2015). Experimental and numerical study of fluid flow and heat transfer characteristics in microchannel heat sink with complex structure. Energy Conversion and Management, 105, 848–857. https://doi.org/10.1016/j.enconman.2015.08.042*

[13] *Wang, H., Chen, Z., & Gao, J. (2016). Influence of geometric parameters on flow and heat transfer performance of micro-channel Heat sinks. Applied Thermal Engineering, 107, 870–879. https://doi.org/10.1016/j.applthermaleng.2016.07.039*

[14] *Xu, B., Ooi, K. T., Mavriplis, C., & Zaghloul, M. E. (2002). Evaluation of viscous dissipation in liquid flow in microchannels. Journal of Micromechanics and Microengineering, 13(1), 53–57. https://doi.org/10.1088/0960-1317/13/1/308*

[15] *Hajmohammadi, M. R., Bahrami, M., & Ahmadian-Elmi, M. (2021). Thermal performance improvement of microchannel heat sinks by utilizing variable cross-section microchannels filled with porous media. International Communications in Heat and Mass Transfer, 126, 105360. https://doi.org/10.1016/j.icheatmasstransfer.2021.105360*